

## OPTIMIZATION OF HOPKINSON BAR INSTRUMENTATION FOR TESTING OF CELLULAR AND LOW IMPEDANCE MATERIALS

J. Falta\*, T. Fíla\*\*, M. Adorna\*\*, P. Zlámal\*\*

**Abstract:** *In this paper, an implementation of Split Hopkinson Pressure Bar (SHPB) and its modification Open Hopkinson Pressure Bar (OHPB) for testing of cellular structures is presented. Dynamic testing of materials with low mechanical impedance is very demanding in terms of achieving the requested experimental device performance. Key elements of the Hopkinson bar instrumentation that were successfully employed in dynamic testing of cellular materials are presented in this paper. Detailed overview of the strain-gauges instrumentation including our best practices for installation and noise reduction is provided. Information about the instrumentation of Hopkinson bar with high-speed cameras are also given. To demonstrate the performance of the proposed instrumentation some examples of a typical results are summarized in the text.*

**Keywords:** SHPB, OHPB, instrumentation, strain-gauge measurement, high speed camera.

### 1. Introduction

Hopkinson Bar is a well-established method for dynamic testing of materials (Wang, et al., 2014). In our lab, two experimental setups are currently used - conventional SHPB and direct impact OHPB. The schemes of the both setups is shown in Fig. 1.

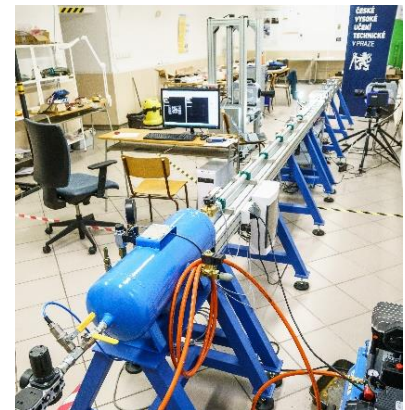
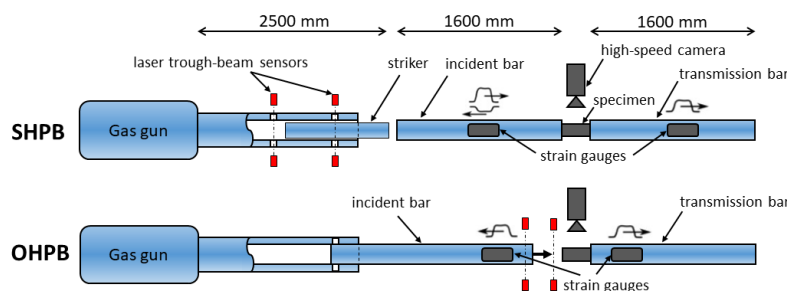


Fig. 1: SHPB/OHPB assembly (left), overview of the experimental setup (right).

Considering the identical gas-gun performance, with the SHPB it is possible to conduct the experiments at higher strain-rates while with OHPB it is possible to reach higher maximal strain in the specimen. For measurements of cellular structures in our case, aluminium and poly-methyl methacrylate (PMMA) bars are employed. Both experimental setups are suitable for testing of porous materials with low mechanical impedance and allow for reaching sufficient strain and strain-rate in the specimen (Yang, et al., 2013, Hou, et al., 2012). However, it is necessary to optimize the individual parts of the instrumentation in order to achieve the required performance with the representative quality and reliability of the recorded data. In this

\* Ing. Jan Falta: Czech Technical University in Prague, Faculty of Transportation Sciences, Department of Mechanics and Materials, Konviktská 20, 120 00 Prague 1, CZ, falta@fd.cvut.cz

\*\* Czech Technical University in Prague, Faculty of Transportation Sciences, Department of Mechanics and Materials, Konviktská 20, 120 00 Prague 1, CZ

paper, description of the custom-developed Hopkinson bar instrumentation (particularly strain-gauges, high-speed cameras and data acquisition system) together with calibration procedures and noise reduction procedures are summarized. Functionality of the instrumentation is demonstrated using the examples of the representative results. Thus, the paper can provide a viable information for the adapting of the Hopkinson bar apparatus for measurement of cellular structures.

## 2. Materials and methods

### 2.1. Strain gauges

In our experimental setups, foil strain gauges (3/120 LY61, HBM, Germany, max. 50,000  $\mu\epsilon$ ) with linear characteristic and semiconductor strain gauges (AFP-500-090, Kulite, USA, max. 1,000  $\mu\epsilon$ ) are used. As the foil strain-gages have significantly lower sensitivity factor (ca. 2 compared to ca. 140 of semiconductors) it is necessary to amplify the foil strain-gauge signal before its digitization. Therefore, it is necessary to maximize the signal-to-noise ratio of the output signal from the foil strain-gauges. Thus, noise reduction is a key factor in strain-gauge instrumentation. In-house twisted pairs wiring with length of individual twists approx. 3 mm is used. Low viscosity cyanoacrylate adhesive (Z70, HBM, Germany) is used for bonding the strain gauge on the bar. Strain-gauges are connected in Wheatstone half-bridge arrangement using the in-house strain-gauge measurement unit (Falta et al., 2018). The force calibration of all strain gauges is carried out after their mounting. The loadcell is mounted between the measurement bars and the bars are subjected to quasi-static load increments using a mechanism with a loading screw. A record of the force (evaluated from strain gauges using known mechanical properties of the bars) from calibration procedure is shown in Fig. 2. Applied load was stepwise increased by 100 N and hold on reached level for 10 s. Installation procedure of the foil strain gauge on the aluminium bar is shown on Fig. 2.

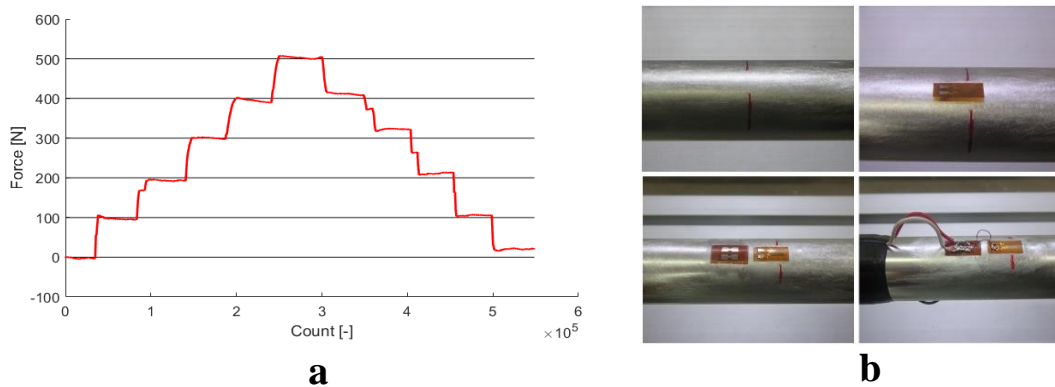


Fig. 2: a) Foil strain gauge calibration on a PMMA bar. b) Foil strain gauge installation procedure: treated surface of the bar (top left), mounting of the strain-gauge (top right), strain-gauge mounted (bottom left), fully installed strain-gauge (bottom right).

### 2.2. High speed cameras

The experiments are observed using a pair of high-speed cameras (FASTCAM SA-Z type 2100K, Photron, Japan) at typical frame-rate in range of 100-300 kfps. During impact testing of cellular materials, it is important to capture sufficient amount of images with suitable resolution for subsequent evaluation using digital image correlation. Resolution of the image decreases with the increasing frame-rate. With our current equipment, it is possible to reach typically 256,000 fps at sufficient resolution, which corresponds to several dozens images of the sample during the impact. The cameras are triggered using a signal from the laser trough-beam photoelectric sensor (FS/FE 10-RL-PS-E4, Sensopart, Germany) as TTL (Transistor-Transistor Logic) synchronization signal at the camera's up-link. This signal is also used as the initial trigger for strain gauge data record and therefore determines the initial time stamp of the record for further synchronization of DIC (Digital Image Correlation) with the strain-gauge (Falta et al., 2018). Selected images representing an important states during the impact compression of the auxetic structure (intact specimen, maximum force and undergoing disintegration) synchronized with the strain gauge signal are shown in fig. Fig. 3-left. Setup with the high-speed cameras is shown in Fig. 3-right.

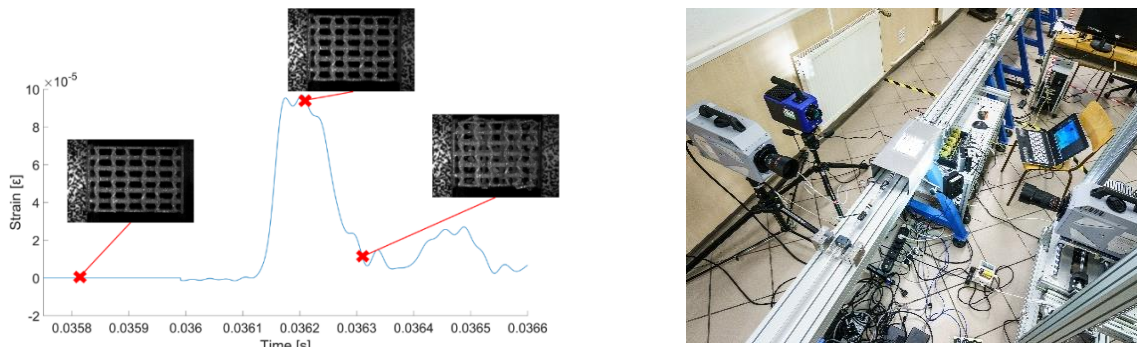


Fig. 3: High-speed images synchronized with the strain-gauge data (left), overview of the Hopkinson bar instrumentation (right).

### 3. Results

With the instrumentation in detail described in the abovementioned section, it was possible to significantly improve the quality and reliability of the measured data. In Fig. 4a the noise levels of strain-gauge signals before and after implementation of the custom twisted-pair wiring are compared. The noise of the signals with custom twisted pairs is approx. 4 times lower that was not possible using commonly available cables (even with versions for strain-gauge measurements). Another important result can be seen in Fig. 4b, where non-filtered signal of the semiconductor and foil strain-gauge signals are compared. Note, that because of its non-linearity the semiconductor strain-gauge starts to exhibit invalid strain-values above approx. 500-1,000  $\mu\epsilon$ . As the amplitudes of the stress-waves in the bars are generally much higher, it is more beneficial to use abovementioned custom twisted-pair cables with foil strain-gauges that provide results with similar precision, high linearity and better lifetime.

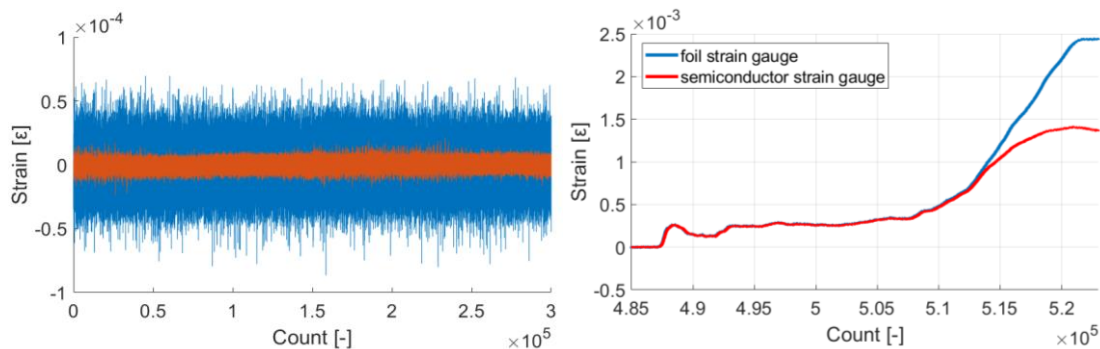


Fig. 4: a) Comparison of noise level with commercial cables (blue) and custom twisted cables (orange).  
b) Comparison of the strain measured by the foil and the semiconductor strain-gauges.

With instrumented cameras as was describe above it is possible to evaluate in-plane displacement, Poisson's ratio or calculate strain fields. Cameras was synchronized with accuracy approx. 2  $\mu\text{s}$ .

### 4. Representative outcomes

Three experiments of the cubic specimens of the closed-cell aluminium foam Alcoras conducted between years 2016-2019 were selected for the demonstration of the improvements in the measurement quality and reliability. As the representative indicator, dynamic equilibrium forces during these experiments were selected and are shown in Figure 5. The different configuration of the measuring device SHPB / OHPB does not have a primary influence on the quality of recorded signal, unlike the realized instrumentation. Thus, the improvement in the quality of the measured force equilibrium can be attributed to the realized wiring and the related parts. In Figure 5a the forces during the experiment in SHPB are shown. Note, that dynamic equilibrium was not achieved as the incident signal is significantly oscillating around the transmission signal and the noise levels are as high as 2 kN. This experiment was not valid. In Figure 5b the results of the experiment conducted in the OHPB are shown. In this experiment the equilibrium was reached and experiment can be considered valid, however the noise levels were still high because of the

wiring (approx. 1 kN) and the reliability of the curves is questionable. In the last experiment (see Figure 5c) OHPB with the custom twisted-pairs was used. Note, that noise levels are significantly reduced, the specimen deforms with dynamic equilibrium and the experiment can be reliably evaluated. Thus, the data can be used for evaluation of stress-strain response of the material at the given strain-rate. Another example of the applicability of a realized experimental device for testing cellular materials is the evaluation of stress-strain and strain-rate-strain curves for 2D re-entrant auxetic structure (see Figure 5d) using OHPB apparatus with the aforementioned instrumentation.

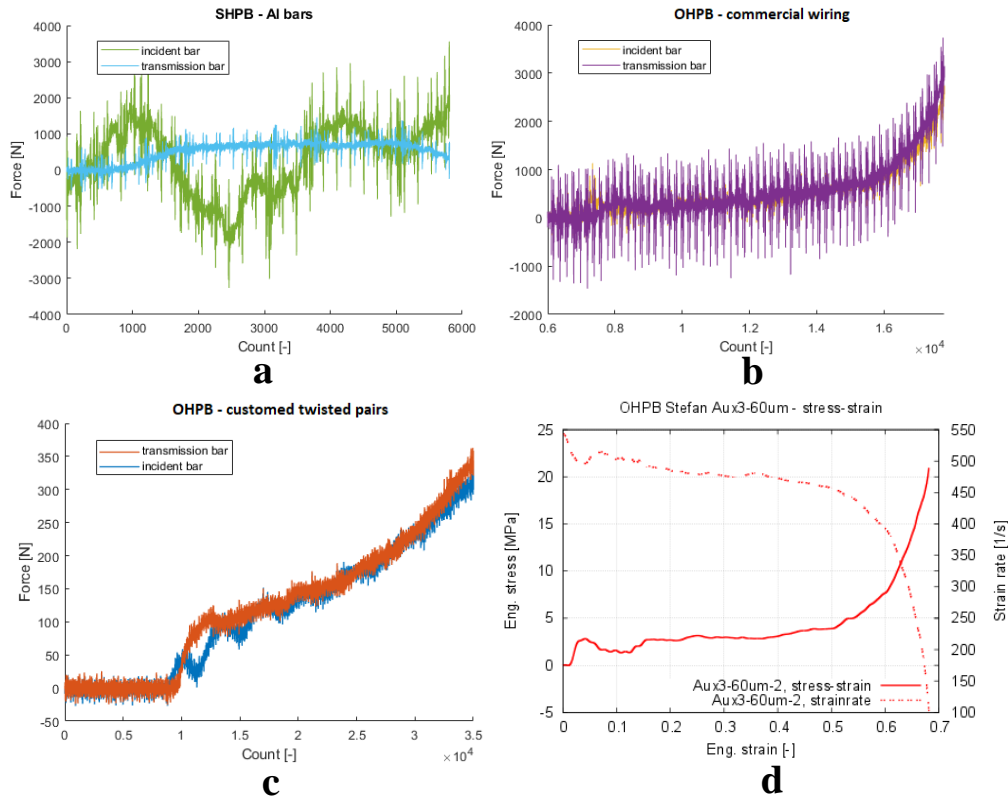


Fig. 5: (a-c) Force equilibrium of the Al-foam in three representative cases. (d) Stress-strain and strain-rate-strain curves for 2D re-entrant auxetic structure.

## 5. Conclusions

Instrumentation of the strain-gauges and the high-speed cameras in the SHPB and the OHPB experimental setups for dynamic testing of the cellular structures was in detail described. The instrumentation allows for measurement of cellular structures with high reliability. Representative results comparing the actual outcomes with the previously conducted experiments exhibiting significant improvements in the quality of the measured data were shown.

## Acknowledgement

The research was supported by the Czech Science Foundation (project no. 19-23675S) and the internal grants of the Czech Technical University in Prague (project no. SGS18/153/OHK2/2T/16 and SGS18/154/OHK2/2T/16). All the financial support is gratefully acknowledged.

## References

- Falta, J, Zlámál, P. Adorna, M. (2018). Instrumentation of Split Hopkinson Pressure Bar for Testing of Cellular Metallic Materials. Acta Polytechnica CTU Proceedings. 18. 10.14311/APP.2018.18.0010.
- Hou B., H. Zhao, S. Pattofatto, et al. Inertia effects on the progressive crushing of aluminium honeycombs under impact loading. International Journal of Solids and Structures 49(19-20):2754–2762, 2012.
- Wang P., S. Xu, Z. Li, et al. Experimental investigation on the strain-rate effect and inertia effect of closed-cell aluminum foam subjected to dynamic loading. Materials Science and Engineering A 620:253–261, 2014.
- Yang B., L. Tang, Y. Liu, et al. Localized deformation in aluminium foam during middle speed hopkinson bar impact tests. Materials Science and Engineering A 560:734–743, 2013.